Original Article

Acteoside protects retinal ganglion cells from experimental glaucoma by activating the PI3K/AKT signaling pathway via caveolin 1 upregulation

Xiaoting Xi[#], Qianbo Chen[#], Jia Ma, Xuewei Wang, Yuan Xia, Xuewei Wen, Bin Cai, Yan Li

Ophthalmology Department, the First Affiliated Hospital of Kunming Medical University, Kunming, China

Contributions: (I) Conception and design: X Xi, Q Chen, Y Li; (II) Administrative support: J Ma, X Wang; (III) Provision of study materials or patients: Y Li; (IV) Collection and assembly of data: X Wen, B Cai, Q Chen; (V) Data analysis and interpretation: Y Xia, Y Li; (VI) Manuscript writing: All authors; (VII) Final approval of manuscript: All authors.

[#]These authors contributed equally to this work.

Correspondence to: Yan Li. Ophthalmology Department, the First Affiliated Hospital of Kunming Medical University, No. 295 Xichang Road, Kunming 650032, China. Email: li_yan_km@163.com.

Background: Glaucoma is the second leading cause of blindness in the world and is characterized by optic neuropathy and degeneration of retinal ganglion cells (RGCs). Our preliminary research found that acteoside can inhibit autophagy-induced apoptosis of RGCs via the phosphatidylinositol 3-kinase (PI3K)/protein kinase B (AKT) signaling pathway. However, it is unclear how acteoside activates the PI3K/AKT signaling pathway to prevents RGCs autophagic apoptosis.

Methods: Animal and cell models were used in this study. Hematoxylin-eosin staining revealed pathological histology of retinas. The number of RGCs in retinas was counted using immunofluorescence. Malondialdehyde and superoxide dismutase were determined using enzyme-linked immunosorbent assay kits. Flow cytometry and terminal deoxynucleotidyl transferase-mediated dUTP nick-end labeling staining were used to detect cell apoptosis. The reactive oxygen species was determined by the Flow cytometry. The proteins were determined by Western blot.

Results: The results showed that acteoside treatment significantly reduced RGC loss, oxidative stress, and autophagy, thereby preventing glaucoma exacerbation. Acteoside reversed caveolin 1 (Cav1) expression and PI3K/AKT signaling activation, according to Western blot results. Cav1 knockdown also reversed acteoside's effects on RGC loss, PI3K/AKT signaling pathway activation, autophagy and oxidative stress. Notably, 3-methyladenine, a PI3K inhibitor, reversed the effects of acteoside and Cav1 overexpression on RGC loss, oxidative stress, and autophagy.

Conclusions: These finding imply that acteoside alleviates RGC loss and oxidative stress by activating of the PI3K/AKT signaling pathway by upregulating Cav1.

Keywords: Acteoside; retinal ganglion cells (RGCs); glaucoma; caveolin 1; PI3K/AKT signaling pathway

Submitted Nov 26, 2021. Accepted for publication Feb 16, 2022.
doi: 10.21037/atm-22-136
View this article at: https://dx.doi.org/10.21037/atm-22-136

Introduction

Glaucoma is the second leading cause of blindness in the world and is characterized by optic neuropathy and degeneration of retinal ganglion cells (RGCs) (1). Although other risk factors, including vascular dysfunction/dysregulation, age, and genetic factors, have also been implicated in the pathophysiology, rise in intraocular pressure (IOP) is a crucial risk factor in the pathogenesis of the disease (2,3). Therefore, lowering of IOP is the main focus during treatment for glaucoma (4). However,

IOP reduction often fails to achieve an ideal outcome since the progressive glaucomatous deterioration of optic nerve function can persist even after treatment (5). Furthermore, a growing body of research indicates that neuroprotective strategies may represent a promising next-generation therapy for glaucoma (6). We previously found that acteoside, a commonly identified phenylpropanoid glycoside in plants, which is the main constituent of Yunnan Ilex latifolia (*Ligustrum purpurascens* Y. C. Yang), rescues glaucoma-induced optic atrophy by preventing autophagic apoptosis of RGCs (7). As artemisinin, metformin and quinine, the natural products from plant, are used by oral or injection. Acteoside is also a plant-based natural product and extract which may be a treatment drug of glaucoma by oral or injection. However, the main molecular mechanism through which acteoside prevents RGCs apoptosis is not yet well understood. Therefore, it is crucial for research to explore the major molecular mechanisms of acteoside in glaucoma.

Acteoside has therapeutic effects in multiple pathological states and has anti-oxidative stress effects (8), anti-inflammatory effects (9), anti-aging effects (10), and anti-RGC loss effects (7). Stress, inflammation, aging, and RGC loss are strongly associated with the pathogenesis of glaucoma (11-13). Hence, acteoside may be a promising protective drug for maintaining homeostasis of RGCs and for preventing glaucoma-related blindness (14,15). Previous studies have suggested that acteoside attenuates oxidative stress, inflammation, and apoptosis by regulating the phosphatidylinositol 3-kinase (PI3K)/protein kinase B (AKT) signaling pathway (7,9,16). The PI3K/AKT signaling pathway has been implicated in many cellular processes (17). An aberrantly activated or inactivated PI3K/AKT signaling pathway has been identified in a variety of human diseases (18). Additionally, researches have shown that the PI3K/AKT signaling pathway is involved in controlling proliferation, apoptosis, and autophagy of RGCs (19-21). Notably, the PI3K/AKT signaling pathway plays an important role in preventing glaucomatous injury-induced loss of RGCs (22). However, how the acteoside activates the PI3K/AKT signaling pathway to prevent autophagic apoptosis of RGCs remains unknown.

Caveolae are flask-shaped vesicular structures located near the plasma membrane, which is abundant in endothelial cells, adipocytes, striated muscle cells, fibroblasts, pneumocytes, and smooth muscle cells (23). Caveolin 1 (Cav1) and 2 (Cav2) are members of the caveolae family (24). In the eye, Cav1 is widely expressed in the majority of retinal cells, including vascular endothelial cells, ciliary epithelia, Muller cells, retinal pigment epithelial cells, photoreceptors, RGCs, and trabecular meshwork (25-27). Cav1 is a scaffold protein on the cell membrane and is associated with signal transduction (28,29). In addition, Cav1 can regulate cell apoptosis, inflammation, and oxidative stress by regulating the PI3K/AKT signaling pathway (30-32). The expression of Cav1 has been shown to increase gradually during the recovery period in retinas after an acute ocular hypertension (HP) injury, but recovery slows down by 7 days after the injury (2). Cav1 expression is downregulated in hydrostatic pressure-induced neuronal cells (33). Furthermore, research shows that Cav1 knockdown can partially protect the inner retinal function in both chronic and acute models of IOP-induced vison loss (34). Hence, Cav1 may be a promising endogenous protective molecule for preventing optic neuropathy and degeneration of retinal ganglion cells in glaucoma. In addition, an *in vitro* experiment showed that acteoside has regulatory effects on Cav1 (35). However, how Cav1 functions in acteoside to prevent loss of RGCs has not been investigated. In this study, we found that Cav1 is downregulated in the RGCs of glaucoma which is upregulated by acteoside treatment. Acteoside inhibits loss of RGCs and oxidative stress and can repair glaucoma by regulating the Cav1/PI3K/AKT signaling pathway. Our preliminary research found that acteoside regulates PI3K/AKT signaling pathway. In this study, we further elucidated the molecular mechanism of acteoside regulates PI3K/AKT signaling pathway by upregulating Cav1. We present the following article in accordance with the ARRIVE reporting checklist (available at https://atm.amegroups.com/article/view/10.21037/atm-22-136/rc).

Methods

Animal model and drug administration

Adult Sprague-Dawley male rats, weighing 220–250 g and 8 weeks old, were obtained from the Hunan SJA Laboratory Animal Co., Ltd. (Certificate no. 43004700043639, China) and housed individually in a temperature-controlled barrier facility with light-dark (12:12) cycles at 22 ℃ with 50% humidity. The rats received *ad libitum* food and water. Experiments were performed under a project license (No. kmmu2021752) granted by the Animal Experimental Ethics Inspection of Kunming Medical University, in compliance with Chinese national guidelines for the care and use of animals. A protocol was prepared before the

study without registration.

The ocular hypertension (HP) animal model was generated by condensing 3 episcleral and limbal veins or the episcleral area of the right eye and sham operation group with conjunctiva incision without coagulation (36). Briefly, rats were sedated with 846 mixture (0.1–0.15 per kg; intramuscular injection). One drop of oxybuprocaine hydrochloride (Santen Pharmaceutical Co. Ltd., Japan) was used to anesthetize the cornea of each rat. Underwater bipolar electrocoagulation was used to rinse and condense the three vorticose veins and limbal veins until the vascular tissue turned white. The rats were randomly divided into the following groups and treated as follows over 8 weeks: (I) sham group; (II) HP group; (III) Act group: HP rats received the acteoside treatment (1 mg/mL; 5 mL acteoside injected into the vitreous); (IV) Act+si-Cav1 (Cav1 small interfering RNA; Guangzhou RiboBio Biotechnology Co., Ltd., Guangzhou, China) group: HP rats received the acteoside and si-Cav1 treatment (diluted in 0.01 M phosphate-buffered saline (PBS); 5 nmol si-Cav1 injected into the vitreous); and (V) Act+3-methyladenine (3-MA, a PI3K inhibitor; Sigma Aldrich, St. Louis, MO, USA) group: HP rats received the acteoside and 3-MA treatment (1.5 mg/kg 3-MA injected into the vitreous). Animals were euthanized at 8 weeks of age, and tissues were harvested for further analysis.

Cell culture and treatment

The RGC-5 cell line was purchased from the Beijing Beina Chuanglian Biotechnology Research Institute (Beijing, China) and cultured in Dulbecco's Modified Eagle's medium (DMEM; Gibco, USA) containing 10% fetal bovine serum (FBS; Gibco) and 1% penicillin and streptomycin (Sinopharm Chemical Reagent, China) at 37 ℃ and 5% CO_2 in an incubator. An RGC-5 IOP *in vitro* model was established as Liu *et al.* previously described (37). The RGCs were exposed to 100 mmHg of hydrostatic pressure. Three different concentrations of acteoside (1, 3, and 5 mg/mL; purity ≥98%, Sigma Chemical Co, MO, USA) or 5 mM 3-MA with different concentrations was added to the cells prior to hydrostatic pressure being applied.

Cell transfection

To construct the Cav1 overexpression vector (oe-Cav1), the Cav1 full-length sequence was inserted into pcDNA3.1 (Invitrogen, USA). Cav1 siRNA (si-Cav1) was synthesized by Guangzhou RiboBio Biotechnology Co., Ltd., (Guangzhou, China). RGC-5 cells (3×10^5) were transfected with 100 nmol of si-Cav1 or oe-Cav1, or were negative controls that used Lipofectamine® 2000 (Invitrogen; Thermo Fisher Scientific, Inc.) following the manufacturer's instructions. After undergoing transfection for 48 hours, the efficiency of transfection was detected by reverse transcription-quantitative polymerase chain reaction (RT-qPCR) and Western blot analysis.

Hematoxylin and eosin (H&E) staining

Eyeballs were harvested and subjected to 4% paraformaldehyde fixation for 24 hours. The tissue blocks were sectioned at 5 μm thickness for subsequent staining. These sections were stained with H&E at room temperature for 10 minutes. Staining of H&E was observed by Nikon Eclipse 80i microscope (Nikon Corporation). Morphological analysis was performed using the ganglion cell layer (GCL) cell density calculation over a distance of 500 μm (100–600 μm) from the edge of the optic disk for three sections from each eye.

Immunofluorescence

After air-drying at room temperature for 30 minutes and being washed in 0.01 M PBS, these sections were permeabilized in 0.5% TritonX-100 and 5% goat serum in PBS for 15 minutes at room temperature. The sections were then incubated overnight at 4 ℃ overnight with rabbit antibodies against brain-specific homeobox/POU domain protein 3A (Brn3a; dilution 1:100; cat. no., ab245230; Abcam, UK). In the next day, Alexa Fluor-conjugated secondary antibodies for 1 hour at room temperature. Finally, the cell nucleus was stained using 0.1% 4'6-diamidino-2-phenylindole (DAPI) for 5 minutes at room temperature. Staining of Brn3a was observed by using a Nikon Eclipse 80i microscope (Nikon Corporation, Japan).

Malondialdehyde (MDA) content and superoxide dismutase (SOD) activity assays

MDA content and SOD activity in retina tissues were measured using their corresponding enzyme-linked immunosorbent assay (ELISA) kits (Jiancheng Bioengineering Institute, Nanjing, China) according to the manufacturer's instructions. Absorbance was determined

using a microplate spectrophotometer (BioTeke, China).

Western blot

The proteins of retina tissues and RGC-5 cells were extracted by using a protein extraction kit (Pierce Biotechnology, USA). Protein concentration was determined using BCAprotein quantification kits (Pierce Biotechnology, USA). The total amount of protein in the supernatant (40 μg/well) was separated by sodium dodecyl sulfate-polyacrylamide gel electrophoresis (10%) and then transferred to a polyvinylidene fluoride membrane after it was blocked in with 5% skimmed milk. Subsequently, the membrane was incubated overnight at 4 ℃ and with 3 Tris-buffered saline (TBS; pH 7.5) wash after each incubation with the following primary antibodies: Cav1 (1:5,000; no. ab2910; Abcam), p-PI3K (1:1,000; no. ab278545; Abcam), PI3K (1:1,000; no. ab133595; Abcam), p-AKT (1:1,000; no. ab38449; Abcam), AKT (1:2,000; no. ab18785; Abcam), LC3 (1:1,000; no. ab192890; Abcam), and β-Actin (1:5,000; no. ab8226; Abcam). These membranes were incubated with goat alkaline phosphatase-labeled anti-rabbit antibody (1:1,000; cat. no. 14708; Cell Signaling Technology, Inc., Danvers, MA, USA). The immunoreactive bands were visualized using an enhanced chemiluminescence reagent (Beyotime Institute of Biotechnology, China). The band intensity was determined with ImageJ software (version 1.47; National Institute of Health, Bethesda, USA).

Detection of cell apoptosis

An Annexin V combined fluorescein isothiocyanate/propidine iodide (FITC/PI; Solarbio, Beijing, China) flow cytometry analysis was used to assess apoptosis. RGC-5 cells were collected in a cold PBS buffer and cultured in the dark for 15 minurtes at room temperature with 10 μL of Annexin V-FITC/PI (1:1). Flow cytometry analysis was then performed using a FACS Verse flow cytometer (Becton Dickinson Biosciences, NJ, USA) and the FlowJo software (version 10; Treestar, OR, USA).

Terminal deoxynucleotidyl transferase-mediated dUTP nick-end labeling (TUNEL) staining

RGC-5 cells were treated or transfected and then cultured for 48 hours with a 2 PBS wash. After this, RGC-5 cells underwent 4% paraformaldehyde fixation for 15 minutes at 37 ℃. 1×10^4 cells were prepared in 96-well plates and then subjected to Click-iT^{TM} Plus TUNEL Assay Kit (ThermoFisher Scientific, Waltham, MA, USA) following the manufacturer's instructions. Following DAPI staining, the apoptotic cells were measured by using a Nikon Eclipse 80i microscope (Nikon Corporation, Japan).

Reactive oxygen species (ROS) analysis

A total ROS detection kit (ThermoFisher Scientific, UK) was used to measure the ROS rate according to the manufacturer's instructions. The cells were incubated with 2',7'-dichlorofluorescein diacetate at 37 ℃ for 25 minutes and with a 3 PBS wash. Finally, a FACS Verse flow cytometer (Becton Dickinson Biosciences, NJ, USA) was applied to analyze the ROS levels at an excitation wavelength of 488 nm and an emission wavelength of 520 nm.

Statistical analysis

All the experiments were repeated three times. All data were statistically analysed and graphed using GraphPad Prism 8 (GraphPad Software, Inc., USA). All data are presented as the mean ± standard deviation. Data between two groups were analyzed using an unpaired Student's *t*-test, and data among multi-groups were analyzed by one-way analysis of variance followed by a Tukey's *post-hoc* test. $P<0.05$ was considered to indicate statistical significance.

Results

Acteoside reduces oxidative stress and RGC loss of retinas

The retinal thickness in three independent groups of rats was measured. As shown in H&E staining, retinas exposed to HP displayed a significant reduced GCL density compared with normal retinas 8 weeks after treatment. The damage to the retina, especially to the GCL, was significantly ameliorated by acteoside (*Figure 1A,1B*). The irreversible apoptosis of RGCs is another important indicator of the functional damage of the retina. Brn3a, an RGC marker, immunofluorescence analysis showed that the number of RGCs was reduced in the retinas at 8 weeks after being HP-exposed compared with normal retinas, and acteoside treatment significantly decreased the extent of RGC apoptosis (*Figure 1C,1D*). The activity of SOD was significantly reduced in the whole retina in subjects exposed to HP compared with control retinas, and SOD was elevated in the acteoside treated-retinas (*Figure 1E*).

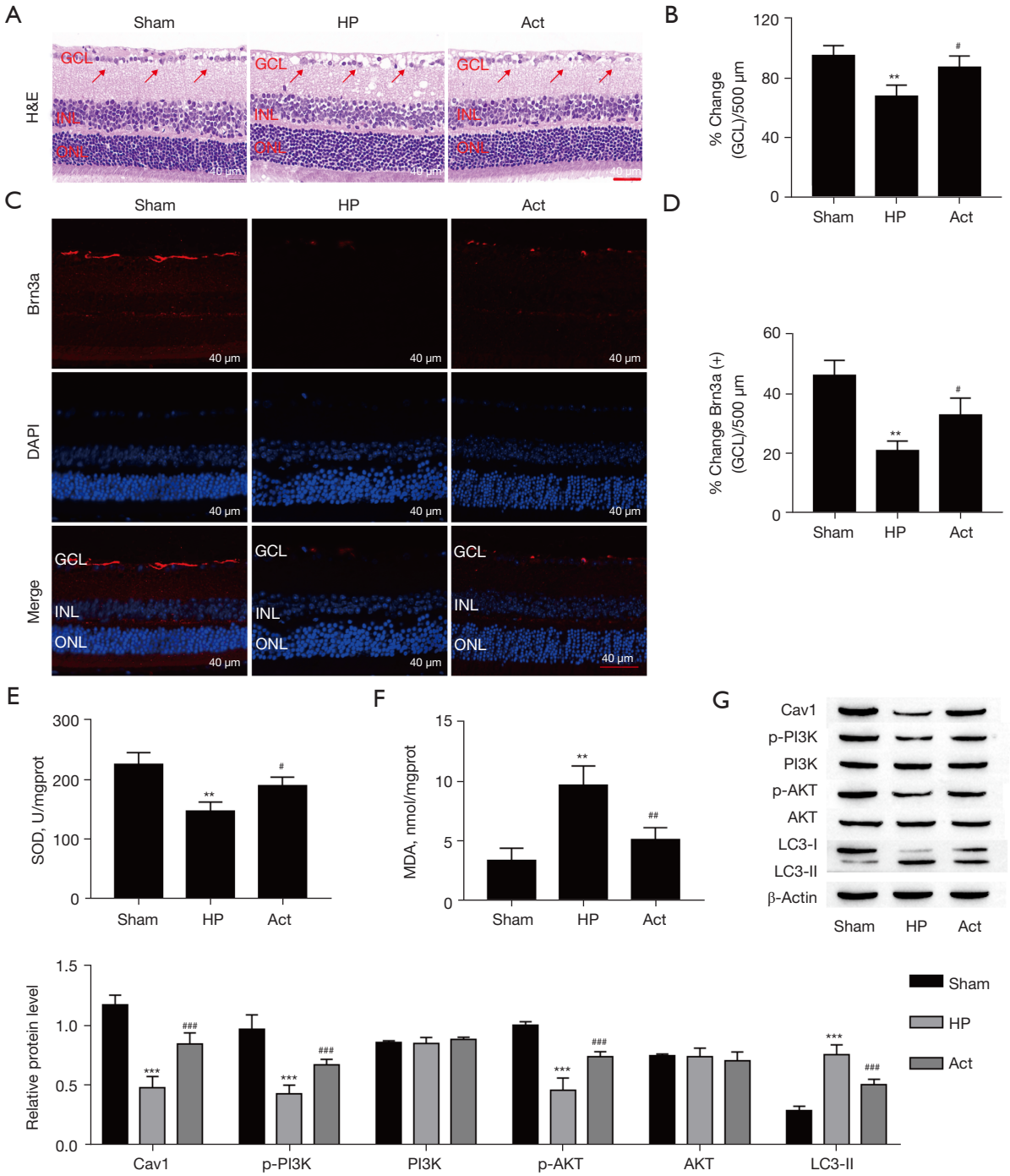

Figure 1 Acteoside reduces oxidative stress and RGC loss of retinas. (A) Representative images of H&E staining. Scale bar =40 μm. (B) Histological analysis GCL counts in retinas (n=3 per group). (C) Expression of Brn3a in GCL cells in retinas. Scale bar =40 μm. (D) Histological analysis RGCs counts in retinas (n=3 per group). (E) SOD activity (n=3 per group). (F) MDA content (n=3 per group). (G) Western blot analysis of Cav1, LC3, and the PI3K/AKT signaling pathway-related protein levels in retinas. **, P<0.01 and ***, P<0.001 *vs.* the sham group; #, P<0.05; ##, P<0.01; and ###, P<0.001 *vs.* the IOP group. The red arrows indicate RGCs. HP, hypertension; Act, acteoside; H&E, hematoxylin and eosin; DAPI, 4'6-diamidino-2-phenylindole; INL, inner nuclear layer; ONL, outer nuclear layer; SOD, superoxide dismutase; Cav1, caveolin 1; PI3K, phosphatidylinositol 3-kinase; AKT, protein kinase B; GCL, ganglion cell layer; MDA, malondialdehyde; RGC, retinal ganglion cell; IOP, intraocular pressure.

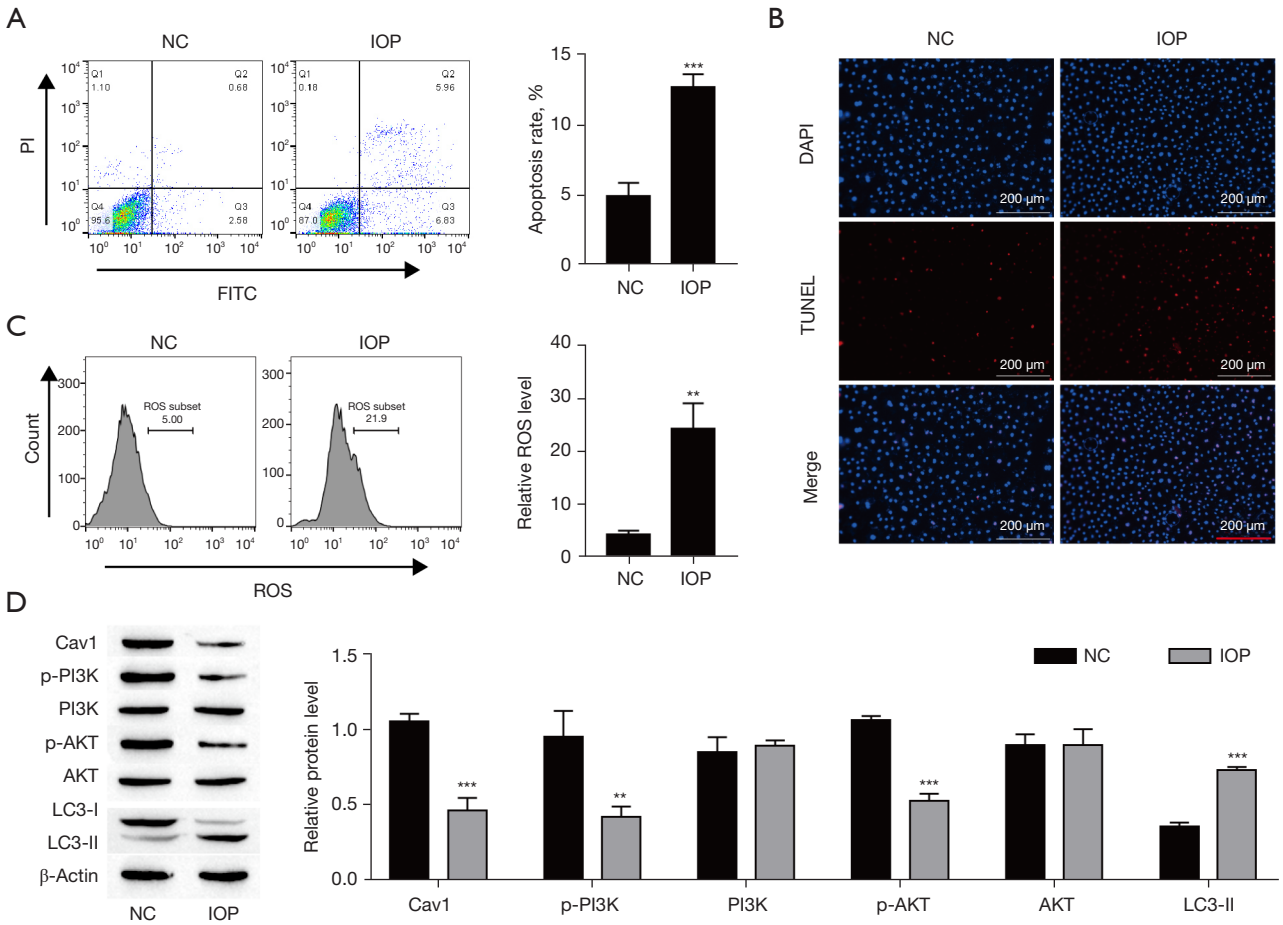

Figure 2 Induced IOP promotes RGC-5 cells injury. (A). Apoptosis of RGC-5 cells detected by flow cytometry. (B). TUNEL staining of RGC-5 cells. Scale bar =200 μm. (C) ROS level of RGC-5 cells detected by flow cytometry. (D) Western blot analysis of Cav1, LC3, and the PI3K/AKT signaling pathway-related protein levels in RGC-5 cells. **, P<0.01 and ***, P<0.001 *vs.* the NC group. NC, negative control; IOP, intraocular pressure; PI, propidine iodide; FITC, fluorescein isothiocyanate; DAPI, 4'6-diamidino-2-phenylindole; TUNEL, terminal deoxynucleotidyl transferase-mediated dUTP nick-end labeling; ROS, reactive oxygen species; Cav1, caveolin 1; PI3K, phosphatidylinositol 3-kinase; AKT, protein kinase B; RGC, retinal ganglion cell.

In contrast, the content of MDA was significantly elevated in the whole retina that was exposed to HP compared with control retinas (*Figure 1F*). Previous studies have shown that acteoside significantly increased Cav1 expression and activated the PI3K/AKT signaling pathway (7,35). As shown in *Figure 1G*, HP exposure lowered the expression of Cav1, p-PI3K, and p-AKT, and all three of these were elevated in the retinas treated with the acteoside treatment. In contrast, LC3-II protein expression was elevated after HP was induced but reduced with the acteoside treatment. These data indicate that acteoside exerts neuroprotective effects against IOP-induced retinal damage.

IOP promotes RGC-5 cells injury

Next, *in vitro* studies were conducted to explore whether IOP could promote injury of RGCs. Compared with the negative control (NC) group, IOP increased cell apoptosis (*Figure 2A,2B*) and ROS level (*Figure 2C*). In addition, the Cav1 expression and the activation of the PI3K/AKT signaling pathway was explored. As shown in *Figure 2D*, IOP reduced Cav1, p-PI3K, and p-AKT expression. Interestingly, LC3-II protein expression was also elevated. These findings showed that IOP promotes injury of RGC-5 cells.

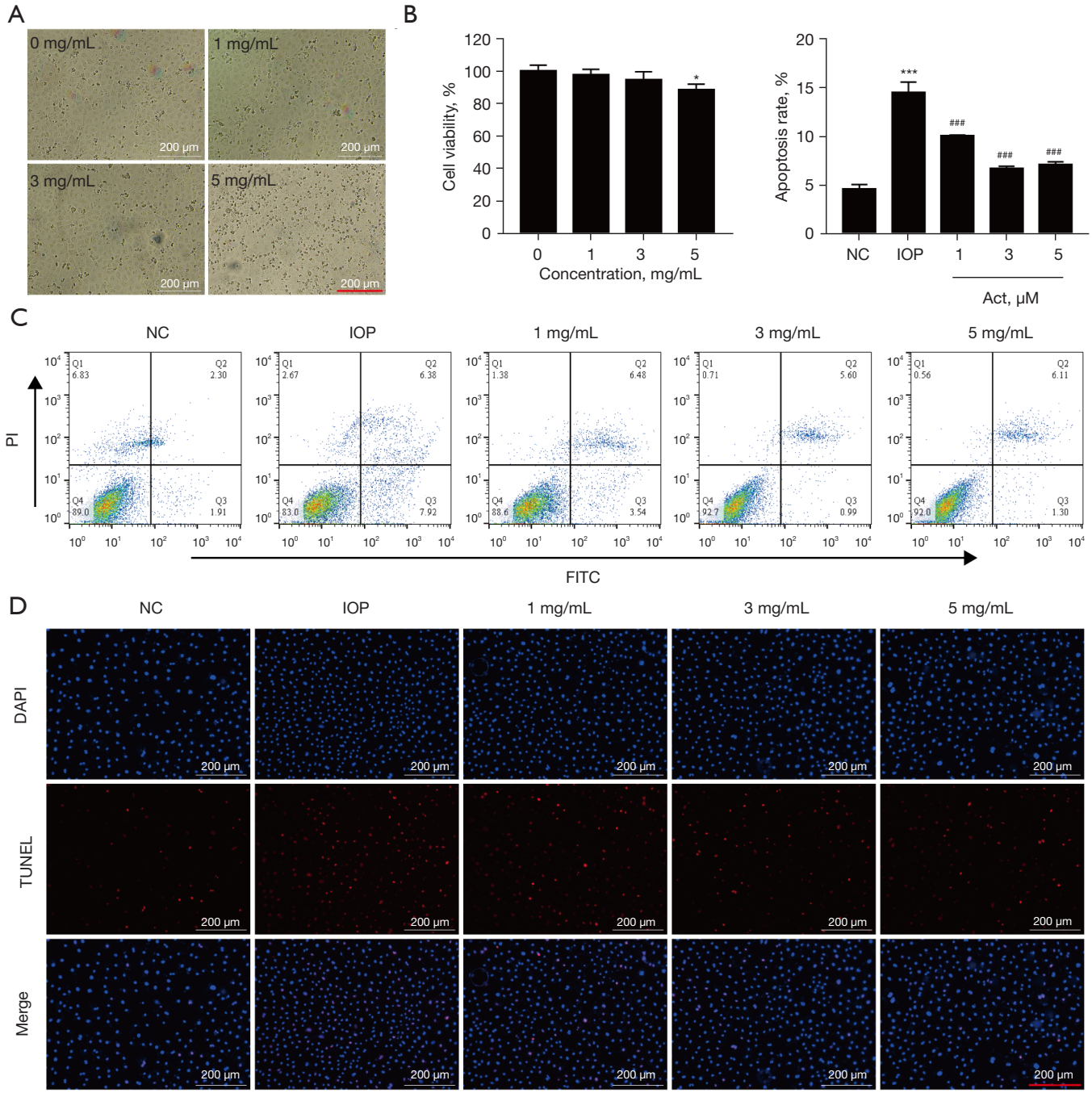

Figure 3 Acteoside relieves cell apoptosis in IOP-induced RGC-5 cells. (A) Microscopic images for acteoside-treated RGC-5 cells at different concentration. Scale bar =200 μm. (B) The viability of RGC-5 cells detected by Cell Counting Kit-8 assay. (C) Apoptosis of RGC-5 cells detected by flow cytometry. (D) TUNEL staining of RGC-5 cells. Scale bar =200 μm. *, P<0.05 *vs.* the 0 mg/mL acteoside. ***, P<0.001 *vs.* the NC group; ###, P<0.001 *vs.* the IOP group. NC, negative control; IOP, intraocular pressure; Act, acteoside; PI, propidine iodide; FITC, fluorescein isothiocyanate; DAPI, 4'6-diamidino-2-phenylindole; TUNEL, terminal deoxynucleotidyl transferase-mediated dUTP nick-end labeling; RGC, retinal ganglion cell.

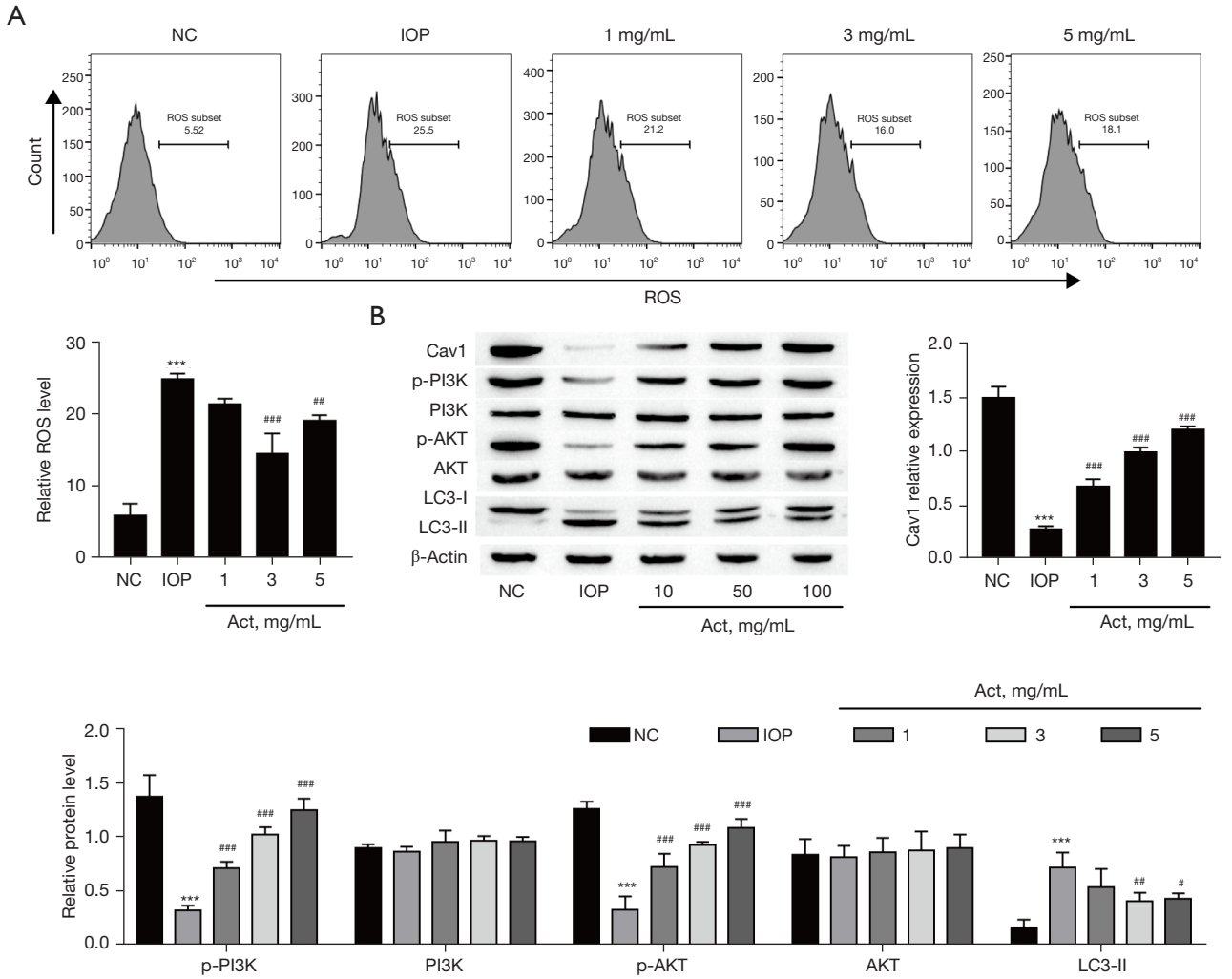

Figure 4 Acteoside relieves oxidative stress and autophagy and elevates PI3K/AKT signaling pathway in IOP-induced RGC-5 cells. (A) ROS level of RGC-5 cells detected by flow cytometry. (B) Western blot analysis of Cav1, LC3, and the PI3K/AKT signaling pathway-related protein levels in RGC-5 cells. ***, P<0.001 *vs.* the NC group; #, P<0.05; ##, P<0.01; and ###, P<0.001 *vs.* the IOP group. NC, negative control; IOP, intraocular pressure; ROS, reactive oxygen species; Act, acteoside; Cav1, caveolin 1; PI3K, phosphatidylinositol 3-kinase; AKT, protein kinase B; RGC, retinal ganglion cell.

Acteoside relieves cell injury in IOP-induced RGC-5 cells

As shown in *Figure 3A,3B*, cell metabolism or proliferation was affected when acteoside concentration reached 5 mg/mL. Therefore, we selected the concentration range from 1 to 5 mg/mL for subsequent *in vitro* studies. IOP increased the apoptosis and ROS levels of RGC-5 cells, and acteoside (1, 3, and 5 mg/mL) treatment decreased the apoptosis and ROS levels (*Figure 3C,3D*; *Figure 4A*). As shown in *Figure 4B*, the protein levels of Cav1, p-PI3K, and p-AKT were decreased after IOP whereas the acteoside treatment remarkably increased the expression of Cav1, p-PI3K, and p-AKT (*Figure 4B*). In contrast, LC3-II protein expression was elevated after IOP but reduced with acteoside treatment. As shown in *Figures 3C,4A*, compared with the 1 mg/mL group, the group treated with 5 mg/mL of acteoside increased the apoptosis and ROS levels. Thus, we chose 3 mg/mL of acteoside for the following cell experiments. These results demonstrated that acteoside decreases IOP-induced RGC-5 cells autophagy, apoptosis, and oxidative stress *in vitro*.

Acteoside relieves cell injury in IOP-induced RGC-5 cells via Cav1

The above results showed that the anti-autophagy, anti-oxidative, and anti-apoptosis effects of acteoside are actively involved in the acteoside-mediated protection of RGCs. A previous study has shown that Cav1 protects RGCs against acute IOP injury by activating the PI3K/AKT signaling pathway (2). Thus, we next determined whether Cav1 and the PI3K/AKT signaling pathway was associated with the acteoside-mediated protection against RGCs apoptosis. To investigate the correlation between Cav1 and RGC injury, the RGC-5 cells were transfected with siRNAs to downregulate Cav1 expression. The protein levels of Cav1 were significantly reduced (*Figure 5A*). si-Cav1-2 achieved more effective knockdown efficiency. The Cav1 depletion significantly decreased the inhibitory effect of acteoside on ROS production and apoptosis (*Figure 5B-5D*). In addition, the expression of Cav1, p-PI3K, and p-AKT was decreased after IOP treatment, but elevated with acteoside treatment, which was finally repressed by Cav1 knockdown (*Figure 5E*). In contrast, IOP elevated the LC3-II level, which was reversed with acteoside treatment, but the LC3-II level was terminally boosted by Cav1 knockdown. Notably, Cav1 depletion significantly blocked the acteoside-medicated neuroprotection against IOP-induced cell injury. This finding indicated that acteoside regulates oxidative stress, apoptosis, and autophagy of RGCs and the PI3K/AKT signaling pathway by upregulating Cav1.

Overexpression Cav1 relieves cell injury in IOP-induced RGC-5 cells by activating the PI3K/AKT signaling pathway

The RGC-5 cells were transfected with oe-Cav1 to increase Cav1 expression. The Cav1 protein level was significantly increased (*Figure 6A*). Notably, Cav1 overexpression attenuated the apoptosis, ROS production, and autophagy of RGC-5 cells after IOP but the inhibitory effects were reversed with 3-MA treatment (*Figure 6B-6D*). In addition, the Cav1 expression was increased with overexpression of Cav1 but was not significantly altered with 3-MA treatment (*Figure 6E*). The level of p-PI3K and p-AKT was reduced after IOP treatment but was reversed with Cav1 overexpression, which was finally repressed by 3-MA treatment (*Figure 6E*). In contrast, IOP elevated the LC3-II level, which was reversed with Cav1 overexpression, but the LC3-II level was terminally boosted by 3-MA treatment. These data suggest that upregulation of Cav1 decreases oxidative stress, apoptosis, and autophagy of RGC-5 cells by activating the PI3K/AKT signaling pathway.

Acteoside relieves IOP-induced RGC loss, oxidative stress, and autophagy through activation of the PI3K/AKT signaling pathway via upregulation of Cav1

Our *in vitro* studies showed that the Cav1/PI3K/AKT axis plays a vital role in acteoside-mediated anti-oxidative, anti-autophagy, and anti-apoptosis effects. We measured the change of retinal thickness in four groups of rats. As shown in H&E staining, acteoside treatment significantly increased GCL density compared with IOP-induced retinas, but the density of GCL was reversed with Cav1 knockdown and 3-MA treatment (*Figure 7A*,*7B*). Immunofluorescence analysis showed that the number of RGCs was elevated in the retinas after acteoside treatment compared with IOP-induced retinas, but the number of RGCs was reversed with Cav1 knockdown and 3-MA treatment (*Figure 7C*,*7D*). The activity of SOD was significantly elevated in the whole retina with acteoside treatment compared with the IOP-induced retina tissues, but the activity of SOD was reversed with Cav1 knockdown and 3-MA treatment (*Figure 7E*). In contrast, the content of MDA was significantly decreased in the whole retina with acteoside treatment compared with the IOP-induced retinas, for which the content of MDA was reversed with Cav1 knockdown and 3-MA treatment (*Figure 7F*). Western blot analysis displayed that the Cav1/PI3K/AKT axis. The level of Cav1 was significantly elevated with acteoside treatment but was reversed with Cav1 knockdown (*Figure 7G*). Acteoside treatment elevated the expression of p-PI3K and p-AKT, but these lowered with Cav1 knockdown and 3-MA treatment. In contrast, LC3-II protein expression was decreased after acteoside treatment but increased with Cav1 knockdown and 3-MA treatment. Taken together, these data indicate that acteoside relieves IOP-induced loss of RGCs, autophagy, and oxidative stress through activation of the PI3K/AKT signaling pathway via upregulation of Cav1.

Discussion

RGCs are the major cellular constituent of the retina, and their loss elevating the risk of eye diseases, including photoreceptor degeneration, diabetic retinopathy, and glaucoma (38,39). Glaucoma is a common, multifactorial neurodegenerative retinal disorder characterized by optic neuropathy and loss of RGCs, which leads to vision loss

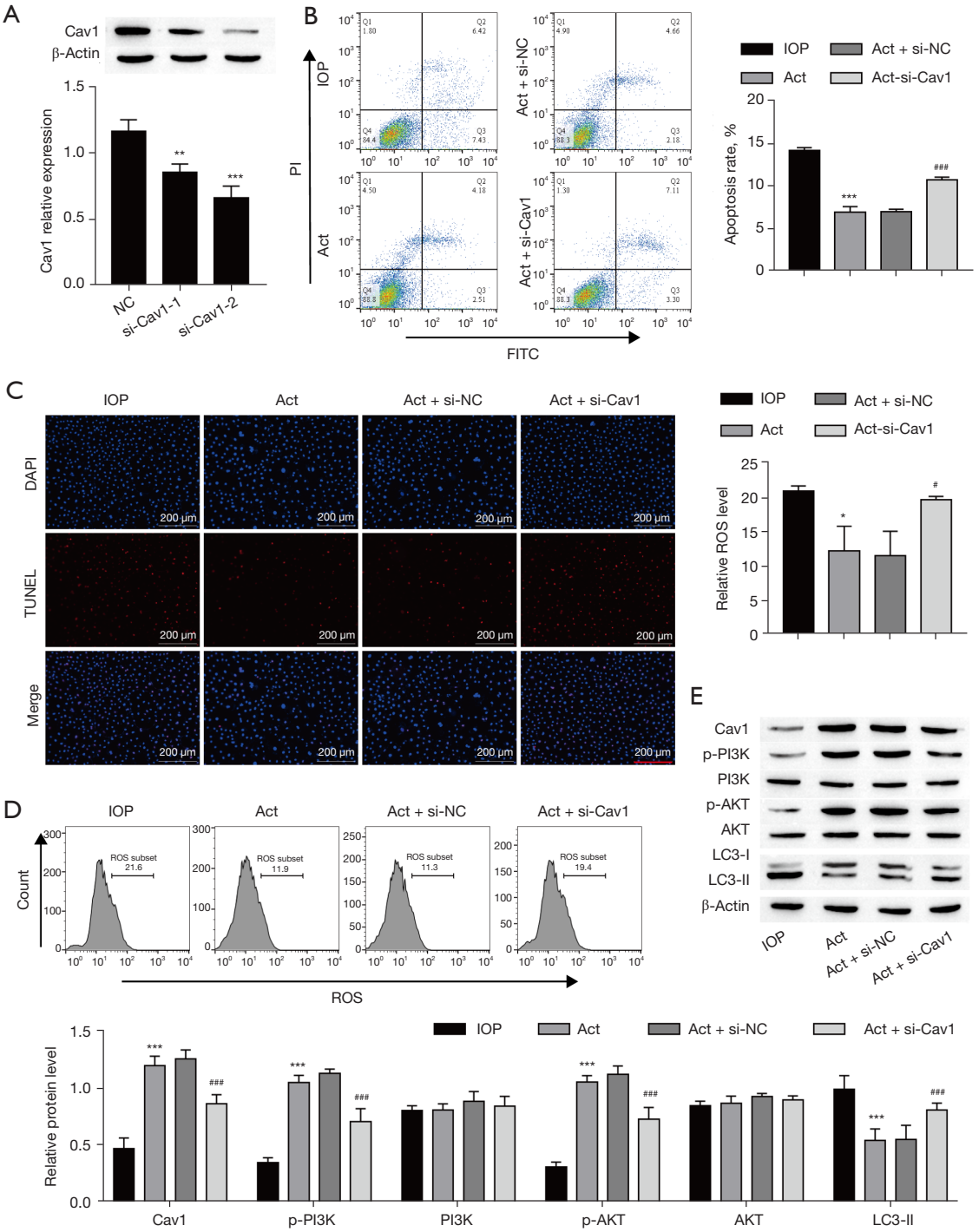

Figure 5 Acteoside relieves cell injury in IOP-induced RGC-5 cells via Cav1. (A) Western blot analysis of Cav1 protein levels in RGC-5 cells. **, P<0.01, and ***, P<0.001 *vs.* the NC group. (B) Apoptosis of RGC-5 cells detected by flow cytometry. (C) TUNEL staining of RGC-5 cells. Scale bar =200 μm. (D) ROS level of RGC-5 cells detected by flow cytometry. (E) Western blot analysis of Cav1, LC3, and the PI3K/AKT signaling pathway-related protein levels in RGC-5 cells. *, P<0.05 and ***, P<0.001 *vs.* the IOP group; #, P<0.05 and ###, P<0.001 *vs.* the Act group. Cav1, caveolin 1; NC, negative control; si, small interfering RNA; IOP, intraocular pressure; Act, acteoside; PI, propidine iodide; FITC, fluorescein isothiocyanate; DAPI, 4'6-diamidino-2-phenylindole; TUNEL, terminal deoxynucleotidyl transferase-mediated dUTP nick-end labeling; ROS, reactive oxygen species; PI3K, phosphatidylinositol 3-kinase; AKT, protein kinase B; RGC, retinal ganglion cell.

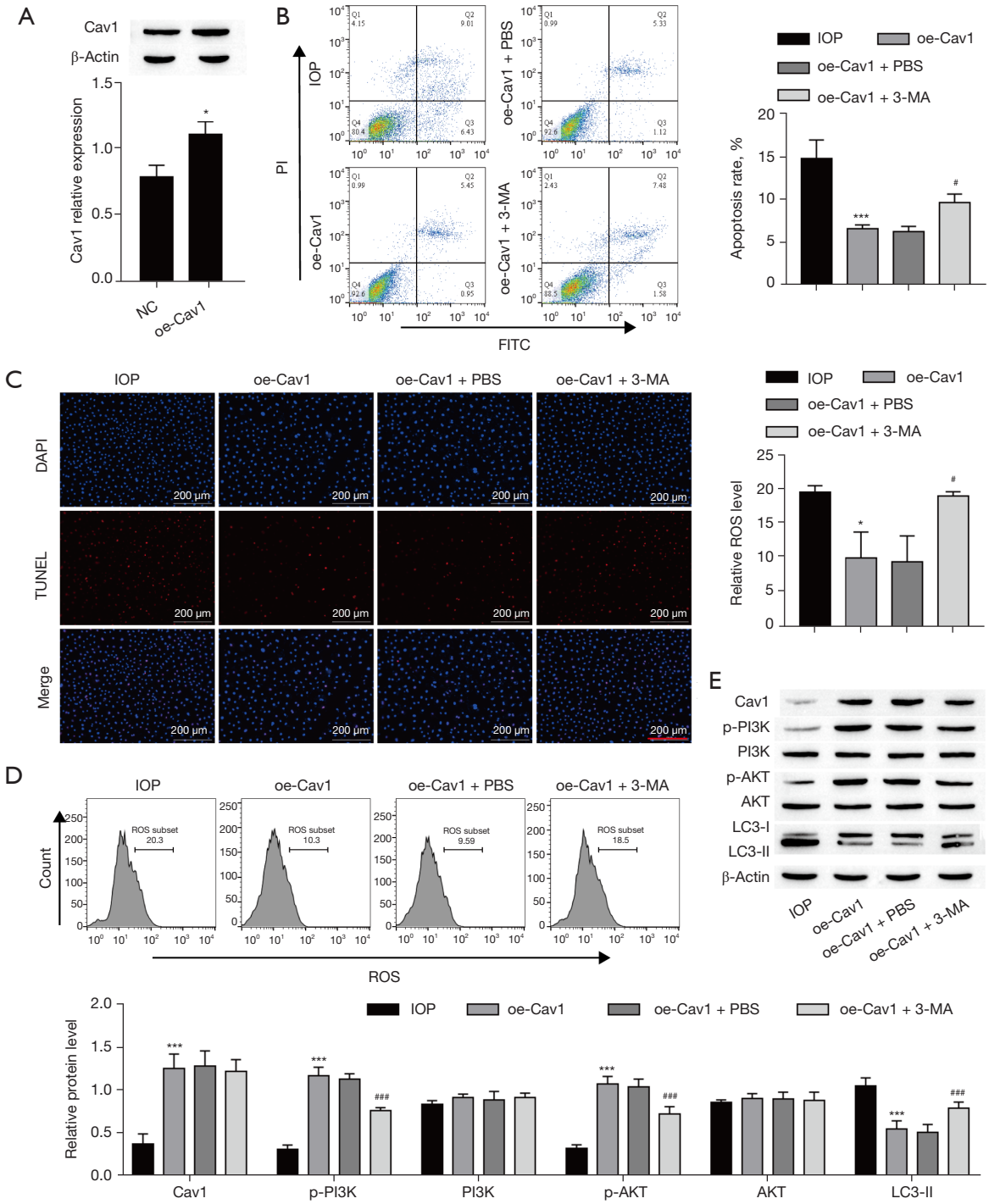

Figure 6 Overexpression of Cav1 relieves cell injury in IOP-induced RGC-5 cells by activating the PI3K/AKT signaling pathway. (A) Western blot analysis of Cav1 protein levels in RGC-5 cells. *, P<0.05 *vs.* the NC group. (B) Apoptosis of RGC-5 cells detected by flow cytometry. (C) TUNEL staining of RGC-5 cells. Scale bar =200 μm. (D) ROS level of RGC-5 cells detected by flow cytometry. (E) Western blot analysis of Cav1, LC3, and the PI3K/AKT signaling pathway-related protein levels in RGC-5 cells. *, P<0.05 and ***, P<0.001 *vs.* the IOP group; #, P<0.05 and ###, P<0.001 *vs.* the oe-Cav1 group. Cav1, caveolin 1; NC, negative control; IOP, intraocular pressure; PBS, phosphate-buffered saline; PI, propidine iodide; FITC, fluorescein isothiocyanate; ROS, reactive oxygen species; PI3K, phosphatidylinositol 3-kinase; oe, overexpression; 3-MA, 3-methyladenine; AKT, protein kinase B; DAPI, 4'6-diamidino-2-phenylindole; TUNEL, terminal deoxynucleotidyl transferase-mediated dUTP nick-end labeling; RGC, retinal ganglion cell.

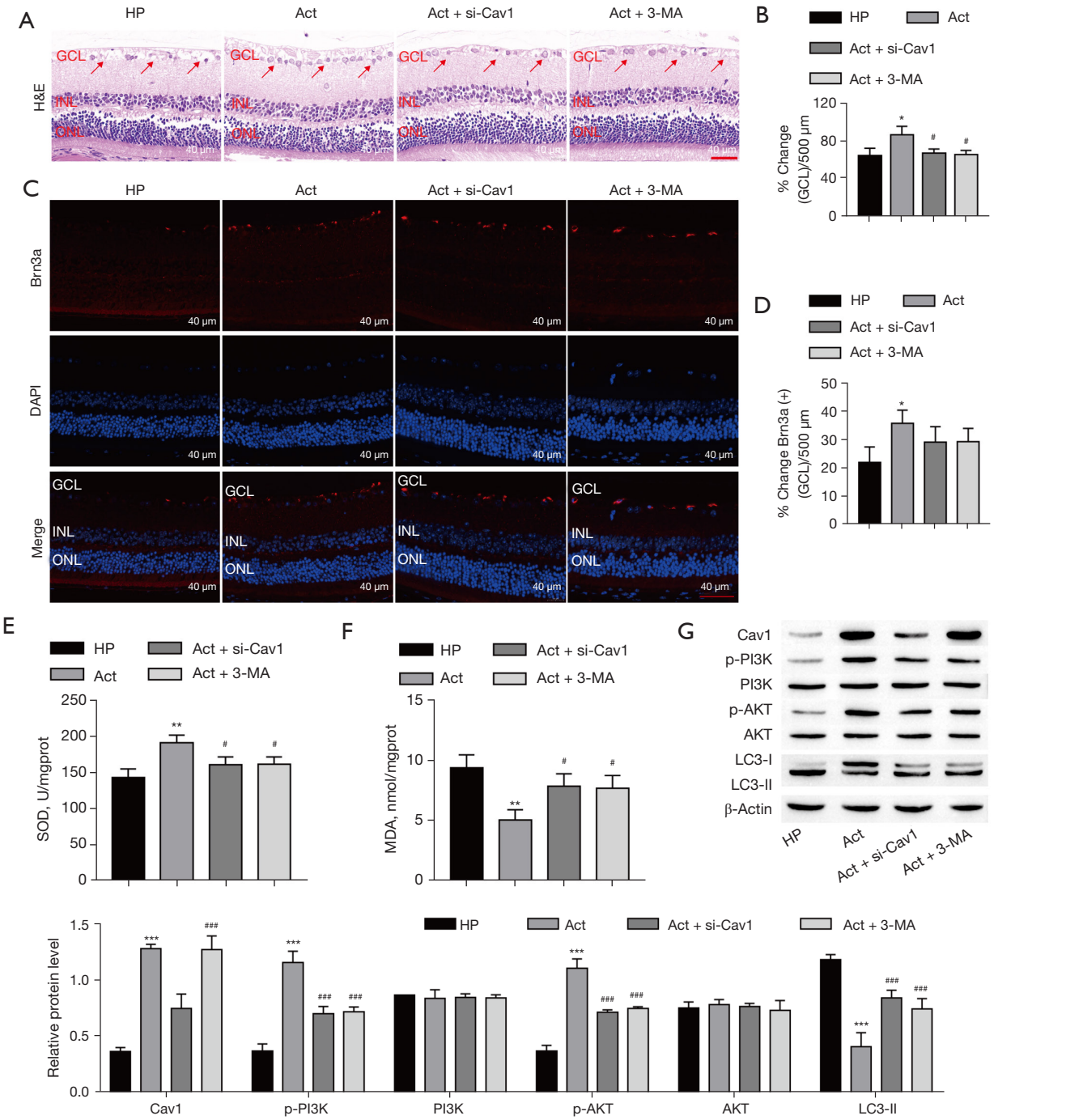

Figure 7 Acteoside relieves IOP-induced RGC loss and oxidative stress through activation of the PI3K/AKT signaling pathway via upregulation of Cav1. (A) Representative images of H&E staining. Scale bar =40 μm. (B) Histological analysis GCL counts in retinas (n=3 per group). (C) Expression of Brn3a in GCL cells in retinas. Scale bar =40 μm. (D) Histological analysis RGCs counts in retinas (n=3 per group). (E) SOD activity (n=3 per group). (F) MDA content (n=3 per group). (G) Western blot analysis of Cav1, LC3, and the PI3K/AKT signaling pathway-related protein levels in retinas. *, P<0.05; **, P<0.01; and ***, P<0.001 *vs.* the Sham group; #, P<0.05 and ###, P<0.001 *vs.* the Act group. The red arrows indicate RGCs. HP, hypertension; Act, acteoside; si, small interfering RNA; 3-MA, 3-methyladenine; H&E, hematoxylin and eosin; IOP, intraocular pressure; GCL, ganglion cell layer; DAPI, 4'6-diamidino-2-phenylindole; INL, inner nuclear layer; ONL, outer nuclear layer; Cav1, caveolin 1; PI3K, phosphatidylinositol 3-kinase; AKT, protein kinase B; SOD, superoxide dismutase; MDA, malondialdehyde; RGC, retinal ganglion cell.

and eventually blindness (40). In our study, a significant loss of RGCs in the retinas of the glaucoma rat's model was observed. Accumulating evidence shows that a neuroprotection strategy would be an effective glaucoma treatment (39,41). Notably, our previous study found that acteoside inhibits autophagic apoptosis of RGCs (7). Here, we also found that acteoside reduced loss of RGCs and RGC-5 cell injury in both *in vivo* and *in vitro* experiments, respectively, suggesting that acteoside exerts neuroprotective functions. These results are consistent with findings that acteoside attenuates oxidative stress-induced neuronal apoptosis in rats with focal cerebral ischemia-reperfusion injury (8). Notably, acteoside has exhibited multiple biological activities *in vitro* and *in vivo*, such as anti-oxidative and anti-apoptotic activities (42). These data suggest that acteoside may function as an anti-oxidative and neuroprotective drug against eye diseases.

Oxidative stress plays an important role in the progress of glaucoma. A previous study showed that the level of MDA increases in the serum and aqueous humor of glaucoma patients, and the activity of SOD is decreased (43). We observed that MDA levels in the retinas of glaucoma rats elevated remarkably, accompanied by an attenuated in SOD activity. Moreover, glaucoma was reported to accelerate the oxidative stress by elevating IOP, thereby increasing oxidative stress-induced death in RGCs, leading to vision loss and eventually blindness (40,44). In our study, we utilized flow cytometry to evaluate the ROS level of RGC-5 cells. The ROS level was significantly elevated in the IOP-induced cells, while acteoside treatment reduced the ROS level. In addition, we utilized flow cytometry and TUNEL staining to evaluate apoptosis of RGC-5 cells. The apoptosis rate was significantly elevated in the IOP-induced RGC-5 cells, while acteoside treatment reduced this value. Furthermore, Western blot data indicated that acteoside treatment reversed the increased expression of LC3-II, suggesting that acteoside can reduce cell autophagy. Existing research has shown that the tight interactions between ROS and autophagy were reflected in the reduction of ROS by autophagy and the induction of autophagy by oxidative stress (45). Here, we further considered oxidative stress-induced autophagy in the RGCs of glaucoma. Accumulating evidence shows that excessive ROS production is associated with many pathological processes (46). We and others have shown that acteoside reduces oxidative stress (7,16,47). Our data support the idea that acteoside may inhibit oxidative stress-linked loss of RGCs, which is beneficial to prevent vision loss and eventually blindness.

Caveolae have been found to play positive roles in maintaining IOP by regulating aqueous humor drainage from the eye (48). Animal experiments have shown that Cav1 is involved in protective effects against IOP-induced eye diseases, including glaucoma (48,49). In this study, we found that the expression of Cav1 decreased in retina tissues of glaucoma model rats; however, acteoside treatment rescued the downregulated expression of Cav1. Notably, acteoside has been shown to increase Cav1 expression in MCF7 cells (35). Acteoside has also been used to increase the activity of PI3K/AKT signaling pathway in various cells and animal models (7,50,51). Furthermore, knockdown of Cav1 expression reversed the effects of acteoside against the oxidative stress, RGC loss, and autophagy, suggesting that Cav1 mediated the protective effects of acteoside against glaucoma. The activation of the PI3K/AKT signaling pathway protects RGCs against various forms of injury in the eye (22). Here, we observed inhibited PI3K/AKT signaling pathway activation in retina tissues of glaucoma rat models; however, acteoside treatment rescued the downregulated activity of the PI3K/AKT signaling pathway. Cav1 knockdown reversed the activator effects of acteoside on the PI3K/AKT signaling pathway. Furthermore, using the 3-MA treatment also attenuated the functions of acteoside against the loss of RGCs, autophagy, and oxidative stress. These results indicated that acteoside relieves loss of RGCs, oxidative stress, and autophagy of glaucoma through activation of the PI3K/AKT signaling pathway by upregulation of Cav1.

Conclusions

Acteoside treatment can significantly protect against the deterioration of eyesight in glaucoma. The protection appears to be largely dependent on the upregulation of Cav1 expression, the activation of the PI3K/AKT signaling pathway, and the inhibition of oxidative stress, loss of RGCs, and autophagy. These results provide a novel molecular mechanism to show how acteoside prevents loss of RGCs in cases of glaucoma.

Acknowledgments

Funding: This work was supported by the Applied Basic Research Fundamental of Yunnan Province [Nos. 2017FE468 (-0175) and 2017FE468 (-046)], the Internal Research Institutions for Scientific Research Projects of Yunnan Medical and Health Institute (grant No.

2018NS0145), the Bethune-Lang Mu Ophthalmological Research Fund for Middle-aged and Young Researchers (grant No. BJLM2017006L), the PhD Innovation Fund of Kunming Medical University (grant No. 2019D011), the National Natural Science Foundation of China (grant No. 82060178), the Doctoral Research Fund of the First Affiliated Hospital of Kunming Medical University (grant No. 2020BS0022), and the Doctoral Innovation Fund Project of Kunming Medical University (grant No. 2019D011).

Footnote

Reporting Checklist: The authors have completed the ARRIVE reporting checklist. Available at https://atm.amegroups.com/article/view/10.21037/atm-22-136/rc

Data Sharing Statement: Available at https://atm.amegroups.com/article/view/10.21037/atm-22-136/dss

Conflicts of Interest: All authors have completed the ICMJE uniform disclosure form (available at https://atm.amegroups.com/article/view/10.21037/atm-22-136/coif). The authors have no conflicts of interest to declare.

Ethical Statement: The authors are accountable for all aspects of the work in ensuring that questions related to the accuracy or integrity of any part of the work are appropriately investigated and resolved. Experiments were performed under a project license (No. kmmu2021752) granted by the Animal Experimental Ethics Inspection of Kunming Medical University, in compliance with Chinese national guidelines for the care and use of animals.

References

1. Quigley HA, Broman AT. The number of people with glaucoma worldwide in 2010 and 2020. Br J Ophthalmol 2006;90:262-7.
2. Zhang L, Xu J, Liu R, et al. Caveolin-1 Protects Retinal Ganglion Cells against Acute Ocular Hypertension Injury via Modulating Microglial Phenotypes and Distribution and Activating AKT pathway. Sci Rep 2017;7:10716.
3. Weinreb RN, Aung T, Medeiros FA. The pathophysiology and treatment of glaucoma: a review. JAMA 2014;311:1901-11.
4. Sihota R, Angmo D, Ramaswamy D, et al. Simplifying "target" intraocular pressure for different stages of primary open-angle glaucoma and primary angle-closure glaucoma. Indian J Ophthalmol 2018;66:495-505.
5. Zhang K, Zhang L, Weinreb RN. Ophthalmic drug discovery: novel targets and mechanisms for retinal diseases and glaucoma. Nat Rev Drug Discov 2012;11:541-59.
6. Almasieh M, Wilson AM, Morquette B, et al. The molecular basis of retinal ganglion cell death in glaucoma. Prog Retin Eye Res 2012;31:152-81.
7. Chen Q, Xi X, Zeng Y, et al. Acteoside inhibits autophagic apoptosis of retinal ganglion cells to rescue glaucoma-induced optic atrophy. J Cell Biochem 2019;120:13133-40.
8. Xia D, Zhang Z, Zhao Y. Acteoside Attenuates Oxidative Stress and Neuronal Apoptosis in Rats with Focal Cerebral Ischemia-Reperfusion Injury. Biol Pharm Bull 2018;41:1645-51.
9. Qiao Z, Tang J, Wu W, et al. Acteoside inhibits inflammatory response via JAK/STAT signaling pathway in osteoarthritic rats. BMC Complement Altern Med 2019;19:264.
10. Peng XM, Gao L, Huo SX, et al. The Mechanism of Memory Enhancement of Acteoside (Verbascoside) in the Senescent Mouse Model Induced by a Combination of D-gal and AlCl3. Phytother Res 2015;29:1137-44.
11. Kimura A, Namekata K, Guo X, et al. Targeting Oxidative Stress for Treatment of Glaucoma and Optic Neuritis. Oxid Med Cell Longev 2017;2017:2817252.
12. Baudouin C, Kolko M, Melik-Parsadaniantz S, et al. Inflammation in Glaucoma: From the back to the front of the eye, and beyond. Prog Retin Eye Res 2021;83:100916.
13. Liu B, McNally S, Kilpatrick JI, et al. Aging and ocular tissue stiffness in glaucoma. Surv Ophthalmol 2018;63:56-74.
14. Wang S, Zeng Y, Li Y. Protective effect on rat retinal ganglion cells and the safety of intravitreal injected acteoside. Chin J Ocul Fundus Dis 2013;29:593-599.
15. Tang Z, Xia Y, Chen Q, et al. The effects of different concentrations of acteoside on the RGC cell model in vitro. Chin J Hypertens 2015;23:1.
16. Peerzada KJ, Faridi AH, Sharma L, et al. Acteoside-

mediates chemoprevention of experimental liver carcinogenesis through STAT-3 regulated oxidative stress and apoptosis. Environ Toxicol 2016;31:782-98.
17. Jafari M, Ghadami E, Dadkhah T, et al. PI3k/AKT signaling pathway: Erythropoiesis and beyond. J Cell Physiol 2019;234:2373-85.
18. Gallyas F Jr, Sumegi B, Szabo C. Role of Akt Activation in PARP Inhibitor Resistance in Cancer. Cancers (Basel) 2020;12:532.
19. Qi Y, Chen L, Zhang L, et al. Crocin prevents retinal ischaemia/reperfusion injury-induced apoptosis in retinal ganglion cells through the PI3K/AKT signalling pathway. Exp Eye Res 2013;107:44-51.
20. Liao R, Yan F, Zeng Z, et al. Amiodarone-Induced Retinal Neuronal Cell Apoptosis Attenuated by IGF-1 via Counter Regulation of the PI3k/Akt/FoxO3a Pathway. Mol Neurobiol 2017;54:6931-43.
21. Yang ZH, Li J, Chen WZ, et al. Oncogenic gene RGC-32 is a direct target of miR-26b and facilitates tongue squamous cell carcinoma aggressiveness through EMT and PI3K/AKT signalling. Cell Biochem Funct 2020;38:943-54.
22. Husain S, Ahmad A, Singh S, et al. PI3K/Akt Pathway: A Role in δ-Opioid Receptor-Mediated RGC Neuroprotection. Invest Ophthalmol Vis Sci 2017;58:6489-99.
23. Sotgia F, Martinez-Outschoorn UE, Howell A, et al. Caveolin-1 and cancer metabolism in the tumor microenvironment: markers, models, and mechanisms. Annu Rev Pathol 2012;7:423-67.
24. Parton RG, del Pozo MA. Caveolae as plasma membrane sensors, protectors and organizers. Nat Rev Mol Cell Biol 2013;14:98-112.
25. Kachi S, Yamazaki A, Usukura J. Localization of caveolin-1 in photoreceptor synaptic ribbons. Invest Ophthalmol Vis Sci 2001;42:850-2.
26. Gu X, Reagan A, Yen A, et al. Spatial and temporal localization of caveolin-1 protein in the developing retina. Adv Exp Med Biol 2014;801:15-21.
27. Berta AI, Kiss AL, Kemeny-Beke A, et al. Different caveolin isoforms in the retina of melanoma malignum affected human eye. Mol Vis 2007;13:881-6.
28. Igarashi J, Michel T. Agonist-modulated targeting of the EDG-1 receptor to plasmalemmal caveolae. eNOS activation by sphingosine 1-phosphate and the role of caveolin-1 in sphingolipid signal transduction. J Biol Chem 2000;275:32363-70.
29. Boscher C, Nabi IR. Caveolin-1: role in cell signaling. Adv Exp Med Biol 2012;729:29-50.
30. Xu Q, Shi W, Lv P, et al. Critical role of caveolin-1 in aflatoxin B1-induced hepatotoxicity via the regulation of oxidation and autophagy. Cell Death Dis 2020;11:6.
31. de Almeida CJG. Caveolin-1 and Caveolin-2 Can Be Antagonistic Partners in Inflammation and Beyond. Front Immunol 2017;8:1530.
32. Kang Q, Xiang Y, Li D, et al. MiR-124-3p attenuates hyperphosphorylation of Tau protein-induced apoptosis via caveolin-1-PI3K/Akt/GSK3β pathway in N2a/APP695swe cells. Oncotarget 2017;8:24314-26.
33. Xu S, Liu S, Yan G. Lycium Barbarum Exerts Protection against Glaucoma-Like Injury Via Inhibition of MMP-9 Signaling In Vitro. Med Sci Monit 2019;25:9794-800.
34. Abbasi M, Gupta VK, Chitranshi N, et al. Caveolin-1 Ablation Imparts Partial Protection Against Inner Retinal Injury in Experimental Glaucoma and Reduces Apoptotic Activation. Mol Neurobiol 2020;57:3759-84.
35. Lv C, Wu X, Wang X, et al. The gene expression profiles in response to 102 traditional Chinese medicine (TCM) components: a general template for research on TCMs. Sci Rep 2017;7:352.
36. Zhao W, Dai L, Xi XT, et al. Sensitized heat shock protein 27 induces retinal ganglion cells apoptosis in rat glaucoma model. Int J Ophthalmol 2020;13:525-34.
37. Liu Q, Ju WK, Crowston JG, et al. Oxidative stress is an early event in hydrostatic pressure induced retinal ganglion cell damage. Invest Ophthalmol Vis Sci 2007;48:4580-9.
38. Levkovitch-Verbin H. Retinal ganglion cell apoptotic pathway in glaucoma: Initiating and downstream mechanisms. Prog Brain Res 2015;220:37-57.
39. Pardue MT, Allen RS. Neuroprotective strategies for retinal disease. Prog Retin Eye Res 2018;65:50-76.
40. Casson RJ, Chidlow G, Wood JP, et al. Definition of glaucoma: clinical and experimental concepts. Clin Exp Ophthalmol 2012;40:341-9.
41. Gossman CA, Christie J, Webster MK, et al. Neuroprotective Strategies in Glaucoma. Curr Pharm Des 2016;22:2178-92.
42. Wu SC, Chen RJ, Lee KW, et al. Angioembolization as an effective alternative for hemostasis in intractable life-threatening maxillofacial trauma hemorrhage: case study. Am J Emerg Med 2007;25:988.e1-5.
43. Benoist d'Azy C, Pereira B, Chiambaretta F, et al. Oxidative and Anti-Oxidative Stress Markers in Chronic Glaucoma: A Systematic Review and Meta-Analysis. PLoS One 2016;11:e0166915.
44. Tanito M, Kaidzu S, Takai Y, et al. Association between systemic oxidative stress and visual field damage in open-

angle glaucoma. Sci Rep 2016;6:25792.
45. Li L, Tan J, Miao Y, et al. ROS and Autophagy: Interactions and Molecular Regulatory Mechanisms. Cell Mol Neurobiol 2015;35:615-21.
46. Brieger K, Schiavone S, Miller FJ Jr, et al. Reactive oxygen species: from health to disease. Swiss Med Wkly 2012;142:w13659.
47. Lee SY, Lee KS, Yi SH, et al. Acteoside suppresses RANKL-mediated osteoclastogenesis by inhibiting c-Fos induction and NF-κB pathway and attenuating ROS production. PLoS One 2013;8:e80873.
48. Elliott MH, Ashpole NE, Gu X, et al. Caveolin-1 modulates intraocular pressure: implications for caveolae mechanoprotection in glaucoma. Sci Rep 2016;6:37127.
49. De Ieso ML, Gurley JM, McClellan ME, et al. Physiologic Consequences of Caveolin-1 Ablation in Conventional Outflow Endothelia. Invest Ophthalmol Vis Sci 2020;61:32.
50. Attia YM, El-Kersh DM, Wagdy HA, et al. Verbascoside: Identification, Quantification, and Potential Sensitization of Colorectal Cancer Cells to 5-FU by Targeting PI3K/AKT Pathway. Sci Rep 2018;8:16939.
51. Yang L, Zhang B, Liu J, et al. Protective Effect of Acteoside on Ovariectomy-Induced Bone Loss in Mice. Int J Mol Sci 2019;20:2974.

(English Language Editor: C. Mullens)

Cite this article as: Xi X, Chen Q, Ma J, Wang X, Xia Y, Wen X, Cai B, Li Y. Acteoside protects retinal ganglion cells from experimental glaucoma by activating the PI3K/AKT signaling pathway via caveolin 1 upregulation. Ann Transl Med 2022;10(6):312. doi: 10.21037/atm-22-136